AD-A133 131 THE REACTION OF CH3O2 WITH NO(U) PENNSYLVANIA STATE 1/1
UNIV UNIVERSITY PARK IONOSPHERE RESEARCH LAB
R SIMONAITIS ET AL. MAR 81 FAA/EE-81-5 DOT-FA79WA-4393
UNCLASSIFIED F/G 7/3 NL

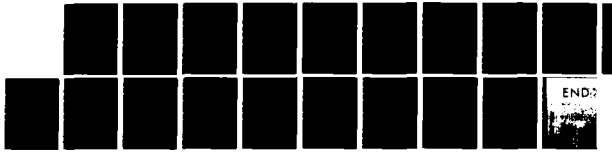

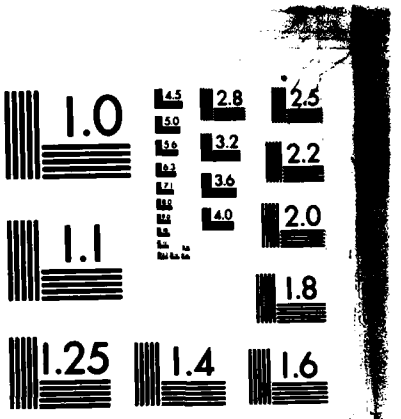

FAA-EE-81-5

13

U.S. Department of Transportation
Federal Aviation Administration

The Reaction of CH_3O_2 with NO

Office of Environment
and Energy
Washington, D.C. 20591

March 1981

R. Simonaitis
J. Heicklen

Technical Report Documentation Page

1. Report No.	2. Government Accession No.	3. Recipient's Catalog No.
FAA-EE-81-5	AD-A133131	

4. Title and Subtitle	5. Report Date
The Reaction of CH_3O_2 with NO	March, 1981
	6. Performing Organization Code
	8. Performing Organization Report No.
7. Author(s)	
R. Simonaitis and Julian Heicklen	
9. Performing Organization Name and Address	10. Work Unit No. (TRAIS)
The Pennsylvania State University University Park, PA. 16802	11. Contract or Grant No. DOT-FA79WA-4393
12. Sponsoring Agency Name and Address	13. Type of Report and Period Covered
U.S. Department of Transportation Federal Aviation Administration Office of Environment and Energy Air Quality Division Washington, D.C. 20591	Final Report September 28, 1979 - September 27, 1980
	14. Sponsoring Agency Code
15. Supplementary Notes	

16. Abstract

The kinetics of reaction 1

$$CH_3O_2 + NO \rightarrow CH_3O + NO_2 \qquad (1)$$

were studied in the temperature range of 218°K to 365°K using the flash photolysis of Cl_2 in the presence of CH_4 and O_2 as a source of CH_3O_2 radicals. These radicals were monitored by ultraviolet absorption. The rate coefficient $k_1 = (2.1 \pm 1) \times 10^{-12} \exp\{(380 \pm 250)/T\}$ cm^3 sec^{-1} at 200 Torr total pressure. The reaction is independent of pressure (70 - 600 Torr, mostly CH_4) at 296°K.

17. Key Words	18. Distribution Statement
Reaction Rates Methylperoxy Radical Nitric Oxide	This document is available to the public through the National Technical Information Service, Springfield, VA 22161

19. Security Classif. (of this report)	20. Security Classif. (of this page)	21. No. of Pages	22. Price
Unclassified	Unclassified		

Form DOT F 1700.7 (8-72) Reproduction of completed page authorized

The Reaction of CH_3O_2 with NO

by

R. Simonaitis and Julian Heicklen

Department of Chemistry and Ionosphere Research Laboratory
The Pennsylvania State University, University Park, Pa., 16802

March, 1981

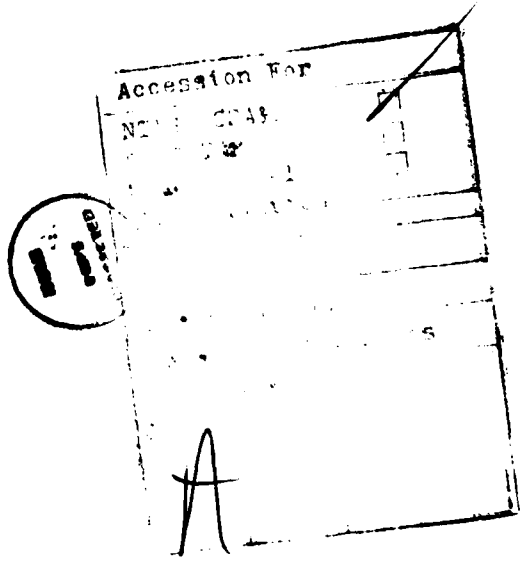

Table of Contents

List of Tables

List of Figures

Abstract

The kinetics of reaction 1

$$CH_3O_2 + NO \rightarrow CH_3O + NO_2 \qquad (1)$$

were studied in the temperature range of 218°K to 365°K using the flash photolysis of Cl_2 in the presence of CH_4 and O_2 as a source of CH_3O_2 radicals. These radicals were monitored by ultraviolet absorption. The rate coefficient $k_1 = (2.1 \pm 1) \times 10^{-12} \exp\{(380 \pm 250/T\}$ $cm^3\ sec^{-1}$ at 200 Torr total pressure. The reaction is independent of pressure (70 - 600 Torr, mostly CH_4) at 296°K.

Introduction

CH_3O_2 radicals are produced in the atmosphere from the oxidation of CH_4. In the stratosphere their principle loss process is the reaction with NO.

$$CH_3O_2 + NO \rightarrow CH_3O + NO_2 \qquad (1)$$

However, in regions of low NO concentration, such as the clean troposphere, reaction 1 may also compete with other CH_3O_2 loss processes (1).

The kinetics of reaction 1 at room temperature has now been measured directly by several groups (2-6). The results of the various studies are summarized in Table I. In general the agreement is good. However, in one study (2) a significantly lower value for k_1 was found, but this has been shown to be incorrect (5). In this paper we report our kinetic measurements of reaction 1 over the temperature range 218-365°K. Since this work was completed, Ravishankara et al have also completed a temperature study of reaction 1 (6, 7).

Experimental

Apparatus

The kinetics of reaction 1 was studied using the flash photolysis-ultraviolet absorption technique. The system consists of four principle parts: the reaction cell, the flash unit, the analysis lamp, and the detection system.

The Pyrex reaction cell with quartz windows is 100 cm long and consists of three concentric chambers with an outside diameter of 5 cm. The inside chamber is 2 cm in diameter and entrance and exit ports at each end provide for the continuous flow of reactants. The flow rate was adjusted such that the mixture was flashed only once to prevent secondary reactions and to reduce NO consumption. Through the middle jacket, cooled or heated fluids were circulated for temperature control. The outside jacket is evacuated for insulation.

A 1 μF capacitor charged to 8-15KV and discharged through two 1-meter long Xe flash lamps placed adjacent to the cell provides the flash radiation. The flash lamp duration at half intensity is ∿15 μs, but the afterglow made measurements possible only after ∿40-50 μs.

A dual beam mode of analysis was employed for increased detection sensitivity. The analysis radiation was from a high pressure 100-watt Hg arc (Oriel Corp.). The collimated beam was passed through a 150 cm long cell containing 1 atm. chlorine to remove radiation that could cause photolysis before being split into analysis and reference beams. Analysis of the effluent for the NO concentration showed no NO removal (±10%) due to the analysis beam.

The analysis beam was detected by an Hamamatsu 1P28 photomultiplier tube after passing through a Bausch and Lomb 33-86-45 monochromator blazed

at 0.3μ with 1200 grooves/mm and having a reciprocal linear dispersion of 1.6 millimicrons/mm. The monochromator was set at 270 nm and the entrance and exit slits were set at 1 mm giving a band pass of 16 nm. The reference beam, after passing through a monochromator was also detected by an Hamamatsu 1P28 photomultiplier tube. The current from the photomultiplier tubes is converted to a voltage pulse which is amplified with a differential pulse amplifier. The output of the amplifier is fed to a Biomation 805 transient recorder interfaced with a Tracor-Northern signal averager. The signal averager output is fed to an Aim 65 microcomputer and the data is stored on tape. With signal averaging, the limiting absorption which can be detected is 4-5 parts in 10^4 with a signal/noise of ∿10. This corresponds to CH_3O_2 densities of ∿3 × 10^{12} cm^{-3} for λ = 270 nm with an absorption cross section σ = 1.5 × 10^{-18} cm^2 (8, 9). Of course since 270 nm is not at the maximum in the CH_3O_2 absorption band, the detection sensitivity for CH_3O_2 at the maximum, (∿245 nm σ = 3.0 × 10^{-18} cm^2) (8, 9) is correspondingly greater. Measurements were made at 270 nm of the CH_3O_2 absorption band rather than at the maximum in order to minimize absorption by the CH_3ONO product.

Materials

Cl_2 (Matheson Research Purity) was purified by passage over KOH and trap to trap distillation. The oxygen (Matheson, extra dry) was used directly from the cylinder. The methane (Matheson, ultra high purity) in some runs was distilled trap to trap, but usually was used without further purification. Its condensable hydrocarbon content was determined to be <30 ppm. The NO (Matheson) was degassed and purified by distillation.

Results

The flash photolysis of Cl_2 in the presence of O_2-CH_4-NO mixtures leads to absorption of 270 nm radiation due to CH_3O_2 production (8-10). A typical absorption decay profile is shown in Figure 1. The important reactions in this system leading to the production of CH_3O_2 and its removal are the following:

$$Cl_2 + h\nu \rightarrow 2Cl \qquad 2$$

$$Cl + CH_4 \rightarrow HCl + CH_3 \qquad 3$$

$$CH_3 + O_2 + M \rightarrow CH_3O_2 + M \qquad 4$$

$$CH_3O_2 + NO \rightarrow CH_3O + NO_2 \qquad 1$$

$$CH_3O + NO \rightarrow CH_3ONO \qquad 5$$

The secondary reactions

$$CH_3O_2 + NO_2 + M \rightarrow CH_3O_2NO_2 + M \qquad 6$$

$$CH_3O + NO_2 \rightarrow CH_3ONO_2 \qquad 7$$

make a small contribution to CH_3O_2 and CH_3O removal. Their effect is considered in the analysis that follows. Reactions of the transients with other species in the system are entirely unimportant due to the relative concentrations of the species involved and their known rate coefficients (7). Cl atoms and CH_3 radicals react on time scales much faster than CH_3O_2.

The measured absorption is due primarily to CH_3O_2 radicals (8-10); however, CH_3ONO contributes to some extent, since the ratio of absorption cross sections $\sigma_{CH_3O_2}/\sigma_{CH_3ONO} = 7$ (9, 11) and since reaction 5 is faster than reaction 1. The absorption due to CH_3ONO is readily apparent in Figure 1 where it can be seen that the baseline does not return to its original value. The cross section for CH_3ONO computed from the final absorption is in the range of (2-5) $\times 10^{-19}$ cm^3 sec which is in agreement

with the literature value (11). The rate coefficient for reaction 5 is 2.2×10^{-11} cm^3 sec^{-1} (13) at 296°K, and assuming a temperature dependence of $(T/300)^{-1.3}$, it is 3.7×10^{-11} cm^3 sec^{-1} at 220°K. Absorption by the product NO_2 and the secondary products $CH_3O_2NO_2$ and CH_3ONO_2 is entirely negligible.

The time dependence of the absorbance, A, due to CH_3O_2 decay and CH_3ONO, NO_2 and other minor product formation is given by

$$\ln(A_0-A_\infty)/(A-A_\infty) = k_1(t-t_0) \qquad \text{I}$$

where t is the time, A_∞ is the limiting absorbance, and A_0 is the initial absorbance after the flash at time t_0. Thus a plot of the left-hand side of equation I vs t will be linear with a slope of k_1. Such a plot is shown in Figure 2, by the dotted line. The slope of this plot gives k_1. Equation I is correct only if $k_5 >> k_1$. If this condition is not satisfied a numerical analysis is required. Since $k_5 \sim (2\text{-}3)k_1$ the error in the determination of k_1 by the use of equation I is expected to be small. Nevertheless a numerical analysis was performed using k_1 obtained from eqn. I above and literature values for k_5, k_6, and k_7. The data computed from these rate coefficients were then plotted in the form of eqn. I as shown by the solid line in Figure 2. This line matches that obtained from the actual data, indicating that eqn. I is valid (otherwise the solid line would have given a larger slope). Thus eqn. I can be used to obtain k_1, and these values are presented in Table II.

The NO concentration introduced into the reaction cell, $[NO]_i$, was corrected for NO consumption and NO_2 production during the relatively long flash tailing period (40-50 μsec) using the first-order relation $[CH_3O_2]_0/[CH_3O_2]_i = \exp(-k_1t_0)$, where $[CH_3O_2]_i$ is the CH_3O_2 concentration just

after the flash, $[CH_3O_2]_0$ is the initial CH_3O_2 concentration at the beginning of the measured part of the reaction and t_0 is the initial time. $[CH_3O_2]_i$ was determined by flashing an identical mixture in the absence of NO. The correction due to NO consumption was small, generally <10%, and the amount of NO_2 present at t_0 was therefore $\lesssim$5% of the initial [NO]. A correction for the amount of CH_3O_2 reacting with NO_2 was applied by converting the NO_2 to an equivalent NO concentration using the known rate coefficients for reactions 1 and 6 (7). Consumption of NO during the course of the reaction was small, generally <10%.

An approximate correction was applied by using the average equivalent NO concentration to compute k_1 from the slopes obtained from a plot of equation I. The error introduced into k_1 by this approximate correction cannot be more than 1-2%, since the values of k_1 computed by using the initial NO concentration and the average equivalent NO concentration differ by $\leq$3%.

Measurements were done at $\sim$218, 296, and 365°K. At 296°K the total pressure was varied by a factor of ten and the initial NO pressure by a factor of 5. k_1 is independent of either variation. The average value of k_1 at 296°K is $(7.7 \pm 0.9) \times 10^{-12}$ cm^3 sec^{-1} where the uncertainty is one standard deviation. At 218°K, k_1 is significantly faster. The average values at $\sim$200 Torr and $\sim$600 Torr total pressure (mostly CH_4) are $(1.3 \pm 0.14) \times 10^{-11}$ and $(1.7 \pm 0.22) \times 10^{-11}$, respectively. The small increase with total pressure may be real, but more accurate measurements are needed to establish this. At 365°K $k_1 = (6.3 \pm 1.0) \times 10^{-12}$ cm^3 sec^{-1}. Values of k_1 at temperatures between 296 and 218°K, were not measured, because it was felt that the precision of the measurements were insufficient to establish the exact shape of the temperature dependence. Instead most of

the effort was put into establishing the value of k_1 at the lower temperature. k_1 can be represented by the Arrhenius expression $k_1 = (2.1 \pm 1) \times 10^{-12} \exp(380 \pm 250/T)$ cm^3 sec^{-1} at $\sim$200 Torr total pressure.

Discussion

Table I summarizes the existing data for k_1. Our measurements at 296°K are in excellent agreement with the recommended value (7).

Sander and Watson's data show a small dependence of k_1 on total pressure, but this is within their experimental uncertainty (5). Our data do not show any pressure dependence at 296°K, but suggest that there may be a very small dependence at 218°K.

Since our work was begun, one other measurement of the temperature dependence of k_1 has been reported. Ravishankara et al (6) find that $E_1/R = -86 \pm 112$°K. While our value of -380 ± 250°K is within their uncertainty limit, there is some disagreement here. A small negative temperature dependence is not surprising, since other reactions of this type such as

$$HO_2 + NO \rightarrow NO_2 + OH$$

$$ClO + NO \rightarrow NO_2 + Cl$$

$$BrO + NO \rightarrow NO_2 + Br$$

exhibit small (100-300°K), negative temperature coefficients (12).

Our temperature dependence corresponds to a temperature coefficient of -1.5. This is exactly the temperature dependence predicted by activated complex theory if the energy barrier is zero and the vibrational partition function is neglected. However inclusion of the vibrational partition function reduces the temperature dependence. Assuming that the four additional vibrations in the activated complex have frequencies of ≈ 600 cm^{-1} associated with nitrite skeletal vibrations (15) gives a temperature coefficient of ≈ -0.9. Likewise the three above-mentioned reactions also show temperature variations that are larger than can be explained.

Thus the magnitude of this negative temperature dependence is not understood, but it is likely at least in part to be associated with the formation of an intermediate complex

$$XO + NO \underset{-a}{\overset{a}{\rightleftarrows}} XONO^* \xrightarrow{b} X + NO_2$$

$$XONO^* + M \underset{-c}{\overset{c}{\rightleftarrows}} XONO + M$$

For XO ≡ HO_2, ClO, or BrO reaction c is not expected to play any role at $\leq$5 atm total pressure (12). However for XO ≡ CH_3O_2 the lifetime of XONO* could be significantly longer and reduce the pressure needed to stabilize XONO to 0.3-3 atm., particularly at lower temperatures. The increased importance of reaction c would also lead to nonlinear Arrhenius behavior which may at least partially reconcile the slightly different temperature dependence observed by us and by Ravishankara et al, because of our substantially larger temperature range. The slight increase in k_1 with pressure at low temperatures is consistent with the stabilization of CH_3O_2NO. However, our data are not sufficiently precise to prove these speculations.

Acknowledgment

This work was supported by the Federal Aviation Administration under Contract No. DOT-FA79WA-4393 for which we are grateful.

References

1. R. Simonaitis, Proceedings of the NATO Advanced Study Institute on Atmospheric Ozone, U. S. Department of Transportation Report No. FAA-EE 80-20 (1979).

2. H. Adachi and N. Basco, Chem. Phys. Lettr., 63, 490 (1979).

3. J. C. Plumb, K. R. Ryan, J. R. Steven and M. F. R. Mulcahy, Chem. Phys. Lettr., 63, 255 (1979).

4. R. A. Cox and G. S. Tyndall, Chem. Phys. Lettr., 65, 357 (1979).

5. S. P. Sander and R. T. Watson, J. Phys. Chem., 84, 1664 (1980).

6. A. A. Ravishankara, F. L. Eisele, N. M. Kreutter, and P. H. Wine, J. Chem. Phys., 74, 2267 (1981).

7. Chemical Kinetic and Photochemical Data for Use in Stratospheric Modelling, National Aeronautics and Space Administration, Jet Propulsion Laboratory Publication 81-3 (1981).

8. C. S. Kan, R. D. McQuigg, M. R. Whitbeck and J. G. Calvert, Intern. J. Chem. Kinetics, 11, 921 (1979).

9. C. J. Hochanadel, J. A. Ghormley, J. W. Boyle and P. J. Ogren, J. Phys. Chem., 81, 3 (1977).

10. E. Sanhueza, R. Simonaitis and J. Heicklen, Intern. J. Chem. Kinetics, 11, 907 (1979).

11. J. G. Calvert and J. N. Pitts, Jr., Photochemistry, Wiley, New York (1966).

12. R. T. Watson, Proceeding of the NATO Advanced Study Institute on Atmospheric Ozone, U. S. Department of Transportation Report No. FAA-EE-80-20 (1979).

13. L. Batt, Intern. J. Chem. Kinetics, 11, 977 (1979).

14. L. Batt and G. N. Rattray, Intern. J. Chem. Kinetics, 11, 1183 (1979).

15. L. J. Bellamy, "The Infrared Spectra of Complex Molecules," John Wiley and Sons, New York (1958) p. 307.

Table I

Summary of measured rate coefficients for $CH_3O_2 + NO \rightarrow CH_3O + NO_2$

Method[a]	P, Torr	$10^{12}A$, $cm^3\ sec^{-1}$	E/R, °K	$10^{12}k(296)$ $cm^3\ sec^{-1}$	Reference
FP-UV	75-100(Ar)	-	-	3.0	2
DF-MS	2-3(Ar)	-	-	8.0 ± 2.0	3
Mol. Mod.	50 (Ar + CH_4) 540 (N_2)	-	-	6.5 ± 2.0	5
FP-UV	75-700 (He)	-	-	7.1 ± 1.4	4
LFP-UV	-	6.3 ± 2.5	-86 ± 112	7.4 ± 1.7	6
Evaluation	-	7.4	0 ± 500	7.4 ± 1.9	7
FP-UV	70-600(CH_4)	2.1 ± 1	-380 ± 250	7.7 ± 0.9	This work

a) FP-UV, flash photolysis-ultraviolet absorption. DF-MS, discharge flow-mass spectrometry; Mol. Mod., molecular modulation; LFP-UV, laser flash photolysis-ultraviolet absorption.

Table II: Flash photolysis of Cl_2-O_2-CH_4-NO mixtures

$[NO]_i$ mTorr	$[NO]_0$ mTorr	$[CH_3O_2]_0$ mTorr	$[M]^a$ Torr	$10^{-12}k_1$, $cm^3\ sec^{-1}$
		T = 218°K, [M] ∿ 200 Torr		
24.9	23.5	1.17	264	12.2
24.1	22.7	0.81	256	10.9
22.0	20.5	0.67	234	12.0
20.1	18.6	0.98	213	13.2
26.4	24.7	1.15	267	12.9
25.3	23.1	0.82	256	14.0
23.7	21.9	0.92	240	13.6
21.7	20.2	0.92	221	15.2
25.6	22.4	1.64	278	14.7
24.6	21.6	1.74	267	15.3
14.4	13.2	1.42	156	14.9
22.6	21.0	1.07	254	14.2
21.2	19.6	1.03	238	11.1
20.5	19.4	0.88	229	15.0
22.4	20.1	2.00	256	14.9
21.4	18.0	1.31	245	12.5
20.4	17.4	1.37	234	13.6
19.5	16.4	1.17	224	12.7
		T = 218°K, [M] ∿ 600 Torr		
23.5	21.1	1.02	660	13.1
21.9	19.8	1.02	616	14.7
19.1	17.5	0.77	572	18.5
17.3	16.4	0.95	518	15.0
22.0	20.1	1.25	554	18.8
19.8	18.0	1.67	589	17.0
17.6	15.1	1.02	512	17.2
18.6	17.0	1.22	660	19.1
17.1	15.6	1.13	605	19.3
		T = 296°K, [M] $\lesssim$ 100 Torr		
11.3	10.9	0.92	60	8.2
11.8	11.4	1.08	130	7.2
12.0	11.6	0.91	132	6.9
20.0	18.8	1.60	96	8.3
21.9	20.9	0.97	106	8.2
25.0	24.0	1.00	121	9.2
27.3	26.5	0.77	132	7.0
27.7	26.2	1.30	134	6.6

Table II concluded

$[NO]_i$ mTorr	$[NO]_0$ mTorr	$[CH_3O_2]_0$ mTorr	$[M]^a$ Torr	$10^{-12}k_1$, $cm^3\ sec^{-1}$
		T = 296°K, [M] $\lesssim$ 100 Torr		
29.1	27.6	1.25	141	7.6
45.6	44.0	0.73	114	8.4
51.6	47.4	1.62	115	8.4
56.7	53.1	1.20	124	6.9
58.2	55.3	0.95	127	7.2
		T = 296°K, [M] $\sim$ 300 Torr		
26.5	25.4	1.14	327	7.2
28.7	27.4	1.07	354	7.2
30.5	29.1	1.07	376	6.8
		T = 296°K, [M] $\sim$ 600 Torr		
16.8	16.0	1.24	540	9.5
18.3	17.3	1.52	589	8.2
21.6	20.2	1.64	567	8.6
21.9	20.9	1.17	561	7.2
23.3	22.3	1.07	610	7.5
		T = 365°K, [M] $\sim$ 200 Torr		
20.6	20.2	0.72	185	5.9
20.6	19.9	0.99	191	4.9
21.8	21.3	0.73	196	7.1
23.0	22.1	1.49	213	5.7
23.4	22.6	1.30	256	6.0
25.3	23.4	1.70	234	7.6
25.5	24.7	1.13	223	5.3
26.5	24.0	1.35	245	8.1
28.9	27.9	0.93	209	5.9

a) $[Cl_2]$ ≈ <2%, $[O_2]$ ≈ 10%, $[CH_4]$ ≈ 88%.

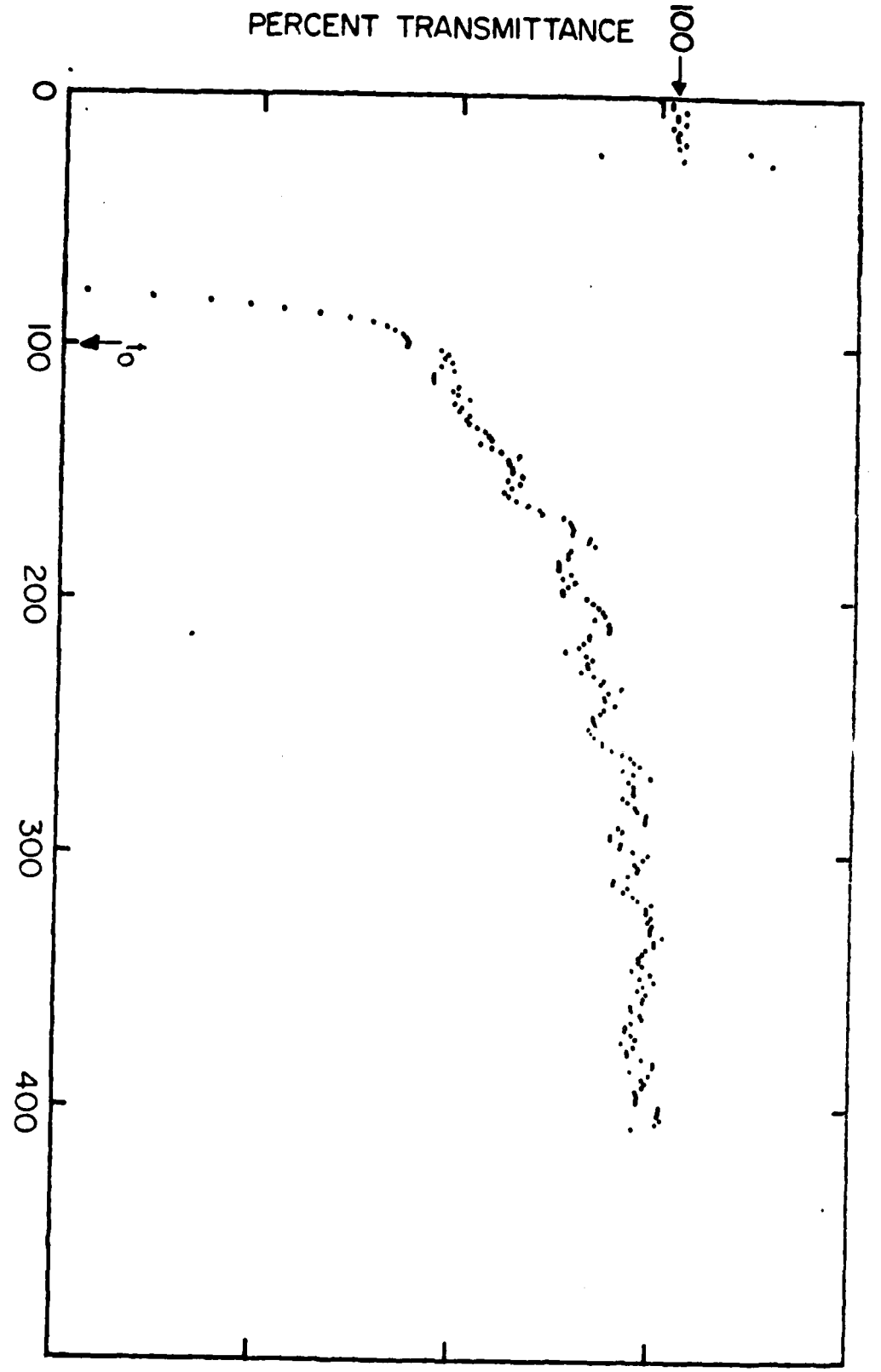

Figure 1. Decay of absorption. $[NO]_0$ = 53.1 mTorr; $[Cl_3O_2]_0$ = 1.2 mTorr. Average of 5 flashes.

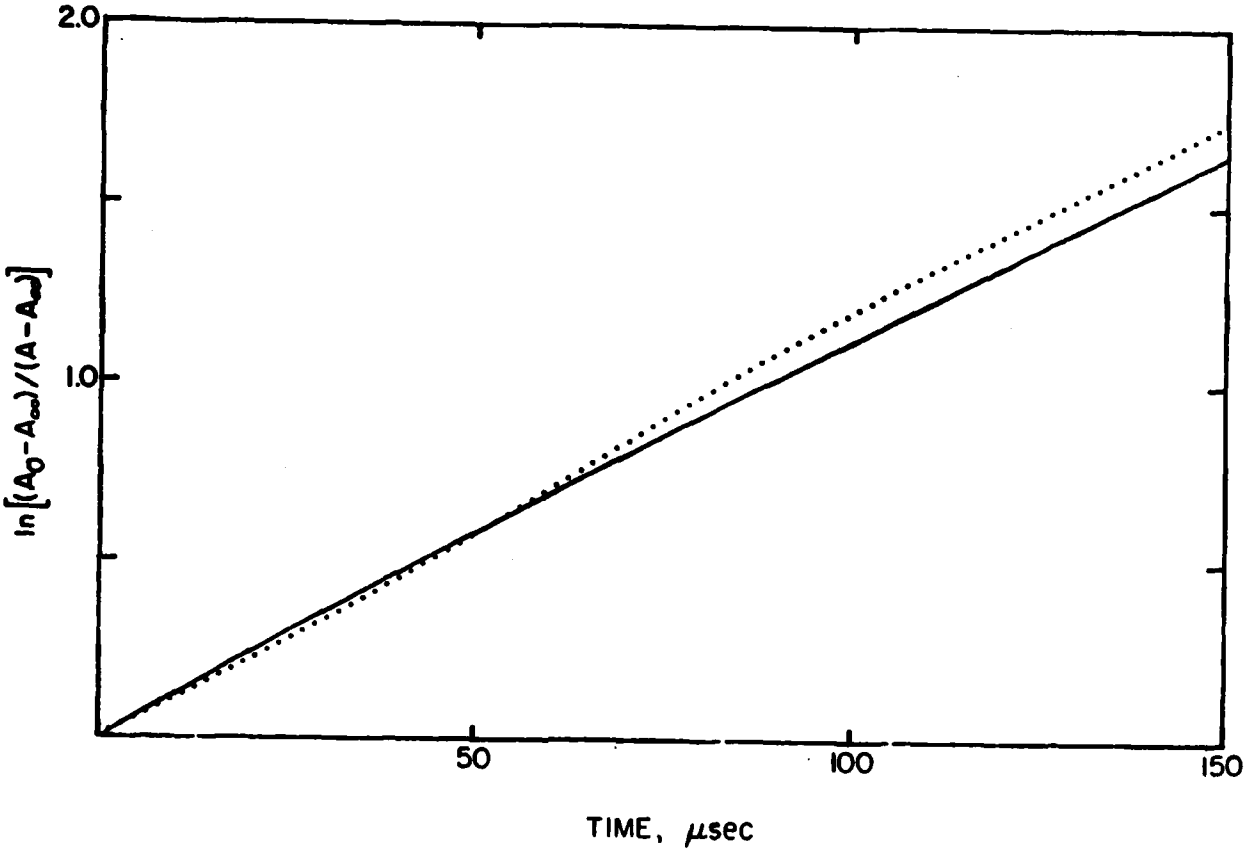

Figure 2. Plot of equation I of the computer smoothed data for the run with $[NO]_0$ = 53.1 mTorr at 296°K (points). Solid line is the computer simulation of this run: $k_1 = 6.9 \times 10^{-12}$ cm^3 sec^{-1}; $k_5 = 2.2 \times 10^{-11}$ cm^3 sec^{-1} (13); $k_6 = 2.5 \times 10^{-12}$ cm^3 sec^{-1} (7); $k_7 = 2.2 \times 10^{-11}$ cm^3 sec^{-1} (14); $\sigma_{CH_3O_2}$ = 1.5×10^{-18} cm^2 (9); $\sigma_{CH_3ONO} = 2 \times 10^{-19}$ cm^2 (11); σ_{NO_2} = 3.1×10^{-20} cm^2 (7).

END

FILMED

10-83

DTIC